Pis'ma v ZhETF, vol. 88, iss. 11, pp. 867 – 872

Hyperactivated resistance in TiN films on the insulating side of the disorder-driven superconductor-insulator transition

T. I. Baturina[1)], *A. Yu. Mironov*, *V. M. Vinokur*[∇], *M. R. Baklanov*[+], *C. Strunk*[*]

Institute of Semiconductor Physics, 630090 Novosibirsk, Russia

[∇] *Material Science Division, Argonne National Laboratory, Argonne, Ill. 60439 USA*

[+] *IMEC, B-3001 Leuven, Belgium*

[*] *Institut für experimentelle und angewandte Physik, Universität Regensburg, D-93025 Regensburg, Germany*

Submitted 28 October 2008

We investigate the insulating phase that forms in a titanium nitride film in a close vicinity of the disorder-driven superconductor-insulator transition. In zero magnetic field the temperature dependence of the resistance reveals a sequence of distinct regimes upon decreasing temperature crossing over from logarithmic to activated behavior with the variable-range hopping squeezing in between. In perpendicular magnetic fields below 2 T, the thermally activated regime retains at intermediate temperatures, whereas at ultralow temperatures, the resistance increases faster than that of the thermally activated type. This indicates a change of the mechanism of the conductivity. We find that at higher magnetic fields the thermally activated behavior disappears and the magnetoresistive isotherms saturate towards the value close to quantum resistance h/e^2.

PACS: 72.15.Rn, 73.50.−h, 74.40.+k, 74.78.−w

The subject of suppression of superconductivity by disorder in thin superconducting films can be traced back to a pioneering work of early forties by Shal'nikov [1], where it was noticed for the first time, that the superconducting transition temperature, T_c, decreases with the decrease of the film thickness. Later, a number of experimental works revealed a drastic suppression in T_c in thin films with the growth of sheet resistance [2 – 4], which is determined by either film composition or thickness and serves as a parameter measuring the degree of disorder. The observed behavior was in a good quantitative accord with theoretical predictions by Maekawa and Fukuyama [5] and the subsequent work by Finkel'stein [6]. The physical picture behind suppressing superconductivity by disorder is that in quasi-two-dimensional systems disorder inhibits electron mobility and thus impairs dynamic screening of the Coulomb interaction. This implies turning on the Coulomb repulsion between electrons which opposes Cooper attraction and, if strong enough, breaks down Cooper pairing and destroys superconductivity. Importantly, according to mechanism of [6], the degree of disorder at which the Coulomb repulsion would balance the Cooper pair coupling is not sufficient to localize normal carriers; thus at the suppression point superconductors transforms into a metal. The latter can be turned into an insulator upon further increase of disorder. Therefore this mechanism, which is referred to as a fermionic mechanism, results in a sequential superconductor-metal-insulator transition [6]. There exists a seemingly alternative picture of the transition, the so-called bosonic mechanism, where the intermediate metallic phase collapses to a single point, implying the *direct* disorder-driven superconductor-to-insulator transition (D-SIT) [7, 8]. Contrary to fermionic mechanism, the bosonic one realizes via localization of the Cooper pairs, which survive even at the nonsuperconducting side of the transition. However, numerical simulations by Ghosal, Randeria, and Trivedi [9] demonstrated that this distinction is not valid: near the D-SIT the homogeneously disordered film breaks up into superconducting islands separated by an insulating sea. Depending on the competition between the charging energy of a single island and the Josephson coupling between the neighboring islands, the film may become either superconducting or insulating, with the island-like structure maintaining at both sides of the transition. Yet the details of the microscopic mechanism of the D-SIT are far from being understood, and uncovering the nature of the phase resulting from suppression of the superconductivity by disorder remains one of the major challenges of condensed matter physics.

In this work we focus on the insulating side of the D-SIT. To begin with, we briefly summarize the up-to-date experimental findings on the subject. In the early

[1)] e-mail: tatbat@isp.nsc.ru

experiments [2] with the very thinnest Pb films it was noticed that once on the nonsuperconducting side, the temperature dependence of resistance acquired an activated character:

$$R = R_0 \exp(T_0/T)\,. \qquad (1)$$

Study of the Bi films [10, 11] revealed three major regimes of the temperature resistance behavior in the insulator domain depending on the degree of disorder. The films closest to D-SIT exhibit comparatively weak insulating trend with conductance lowering as $\log T$ upon decreasing temperature. Moderately disordered films, that are more far from the D-SIT, demonstrate the Efros-Shklovskii (ES) behavior, $R = R_1 \exp[(T_{ES}/T)^{1/2}]$, and the resistance in most disordered films is thermally activated (1). The direct D-SIT was found in InO_x films [12], exhibiting a sequence of temperature behaviors on the nonsuperconducting side: deep in the insulating regime, the conductivity shows Mott's variable range hopping (VRH) [12, 13], on approach to the transition with decreasing disorder it changes to ES law [13], and the films closest to D-SIT shows activation (1), which transforms to Mott's VRH at larger T [13]. Interestingly, the crossover from the activation to ES law, and eventually to Mott's VRH regime was also observed in InO_x composite films [14] upon increasing temperature. It was noticed in Ref. [12] that applying a relatively small perpendicular magnetic field (0.7 T) to the least disordered insulating films results in positive magnetoresistance, while more resistive samples show purely negative magnetoresistance. Gantmakher's group carried out measurements of the effect of the magnetic field up to 20 T on the insulating InO_x films in the vicinity of the D-SIT [15] and revealed nonmonotonic magnetoresistance behavior: a positive magnetoresistance at low magnetic fields turning into a negative magnetoresistance upon increasing the field. Importantly, several works, starting from the earliest [12, 15] and ending by recent [16] demonstrate that in the zero magnetic field the resistance of insulating films closest to the transition deviates *downward* from the Arrhenius activated behavior at lowest temperatures. At high magnetic fields, the charge transfer mechanism appears the same as that at the zero field but high temperatures and follows Mott's VRH law [15]. Another recent finding worth noticing is the dependence of the activation energy in InO_x films on the linear size of the film (the distance between the leads) [17]. The D-SIT in TiN was found for the first time on the films prepared by magnetron sputtering [18]. On the insulating side close to the transition, the resistance exhibited thermally activated behavior till lowest temperatures available. In our preceding works [19, 20], where we were dealing with the thin TiN films grown by atomic layer chemical vapor deposition, an exceptionally sharp D-SIT was found. At zero and low magnetic fields the resistance displayed thermally activated behavior with the nonmonotonic dependence of activation temperature on the magnetic field. Here we present the novel results on identically prepared samples showing that at the lowest temperatures the resistance deviates *upward* from the Arrhenius activated dependence (1) in a contrast to observation in InO_x films [12, 15, 16]. Hereafter we will referring to this behavior as to *hyperactivation*. This behavior holds at low magnetic fields. At higher magnetic fields, instead of this low-temperature upturn, the resistance shows *downward* deviation from the Arrhenius activation. The analysis of the corresponding magnetoresistance shows that it decays exponentially with field towards the finite value close to the quantum resistance $R_Q = h/e^2$.

The resistance was measured by the four-terminal technique in the linear I-V regime even at very low temperatures. The width of the film was 50 μm, the distance between the voltage probes was 100 μm, thus the sample comprised two squares. All the data are presented as resistance per square. The samples were cooled down in the Oxford 200 TLE dilution refrigerator. Magnetic fields up to 10 T were applied perpendicular to the film surface.

We start with the zero magnetic-field results obtained during the cooling the cryostat down from room temperature. Shown in Fig.1a are the temperature dependences of the resistance $R(T)$ of two samples, **S** and **I**. At room temperature, their resistances are close ($R_{300} = 4.48\,\mathrm{k\Omega}$ and $R_{300} = 4.76\,\mathrm{k\Omega}$, respectively), but diverge upon decreasing temperature. Namely, the **S**-sample falls into a superconducting state, whereas the **I**-sample becomes an insulator. Upon cooling down to 3 K both samples exhibit nearly identical logarithmic temperature dependence of the conductance (see inset in Fig.1a), which is well described by the formula $G(T)/G_{00} = A\ln(k_B T\tau/\hbar)$, where $G(T) = 1/R(T)$ is the conductance, $G_{00} = e^2/(\pi h)$, and $A = 2.55$ for both samples. This behavior is in accord with the theory of quantum corrections for quasi-two-dimensional disordered systems and can be attributed to localization and repulsive electron-electron interaction corrections [21]. To characterize the behavior of the **I**-sample at low temperatures we replot $R(T)$ versus $1/T$ in Fig.1b. In the temperature interval between 0.25 and 0.9 K, the resistance is well fitted by a thermally activated dependence of Eq. (1), with $T_0 = 0.63\,\mathrm{K}$ being the activation temperature, and $R_0 \approx 17\,\mathrm{k\Omega}$. Plotting the same data as $\log R$ versus $1/T^{1/2}$ one can see that the resistance can be nicely fitted by the ES-law in the higher temperature

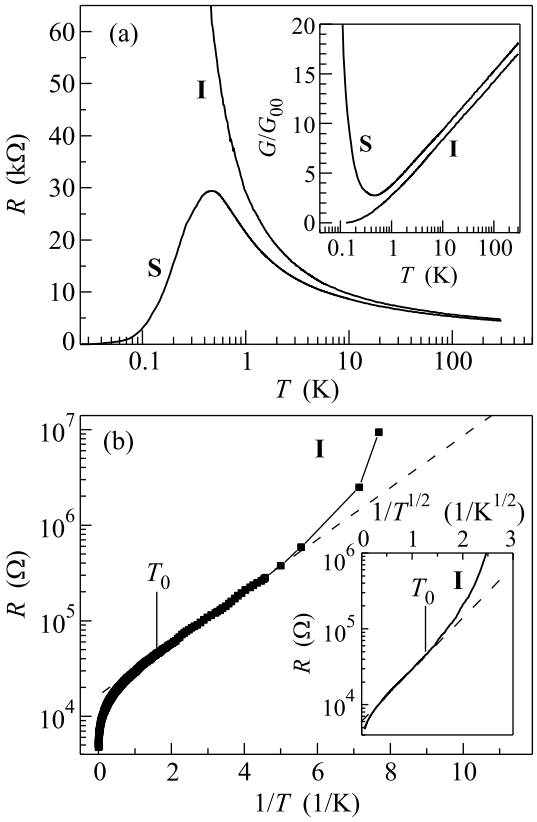

Fig.1. Zero magnetic field temperature behavior of the resistances of samples **S** and **I**. Panel (a): R versus $\log T$ plots for **S** and **I** samples are nearly undistinguishable at high temperatures. The inset: the same data replotted as $G/G_{00} = \pi h/e^2 R$ versus $\log T$ show almost identical logarithmic temperature dependences of both samples in the range 6 – 300 K. Panel (b): $\log R$ versus $1/T$ plot for the **I**-sample displays Arrhenius activation, the activation temperature being $T_0 = 0.63$ K, determined by fit to Eq. (1) the data in the temperature range 0.25–0.9 K. The line bar marks this T_0. At lowest temperatures $\log R(T)$ turns upwards departing from the Arrhenius- to *hyperactivated* regime. The inset: the same data plotted as $\log R$ vs. $1/T^{1/2}$, demonstrate the ES regime wedging in between the logarithmic and activated transport. The fitting parameters are: $T_{ES} = 2.6$ K and $R_1 = 6.2$ kΩ

range 0.6 – 6 K (see inset in Fig.1b). Note, that the deviation from the ES-law towards the activation starts at the temperature $T \lesssim T_0$. To summarize here, the evolution of $R(T)$ of the insulating TiN film in the zero magnetic field is as follows. As temperature decreases, the resistance shows first a logarithmic growth crossing over into the ES-law, which in its turn, transforms into the Arrhenius activated behavior, with all three subsequent regimes pairwise overlapping. So far the temperature behavior of $R(T)$ in TiN films more or less parallels that of InO_x [14, 13]. An important difference arises at the very lowest temperatures where $R(T)$ of TiN shoots up from the Arrhenius dependence contrasting the downturn observed in InO_x [12, 15, 16].

Turning on the magnetic field we find its huge effect on the transport properties of the insulating TiN films (see Fig.2). Even a small ramping of the field from zero

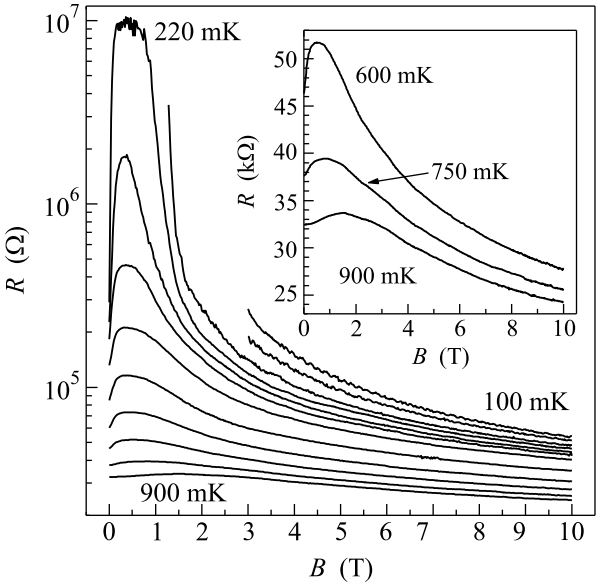

Fig.2. Magnetoresistance isotherms for the sample **I** taken at temperatures T = 100, 140, 190, 220, 240, 260, 300, 380, 480, 600, 750, 900 mK respectively from the top to the bottom. The inset shows a close-up view of the $R(B)$ curves measured at T = 600, 750, 900 mK

to 0.1 T at 220 mK causes at least the 30 times increase in the resistance; more specifically, the resistance grows from $2.9{\cdot}10^5\,\Omega$ to $10^7\,\Omega$, which is the upper limit of the used measuring circuit. The magnetoresistance demonstrates pronounced nonmonotonic behavior: an abrupt raise and rapid drop of the resistance in the window of about 1.5 T wide, the latter transforming into a flattening tail at large fields. At T = 220 mK, the negative magnetoresistance of the insulating sample exceeds two orders of magnitude, and at 10 T resistance drops down to $R = 46$ kΩ. Another interesting feature of the magnetoresistance is a gradual shift of the peak to higher fields upon increasing the temperature. This behavior is clearly seen in the inset showing enlarged images of the subsequent three highest temperature isotherms.

Taking the fixed-field cuts across the data presented in Fig.2, we find that in the temperature range 0.3 – 0.9 K all the $\log R(T, B_i)$ versus $1/T$ plots are linear at all magnetic fields. Thus, making use of the Eq. (1), we have determined field dependences $T_0(B)$ (shown in the inset of Fig.3) and $R_0(B)$ (which vary between 13

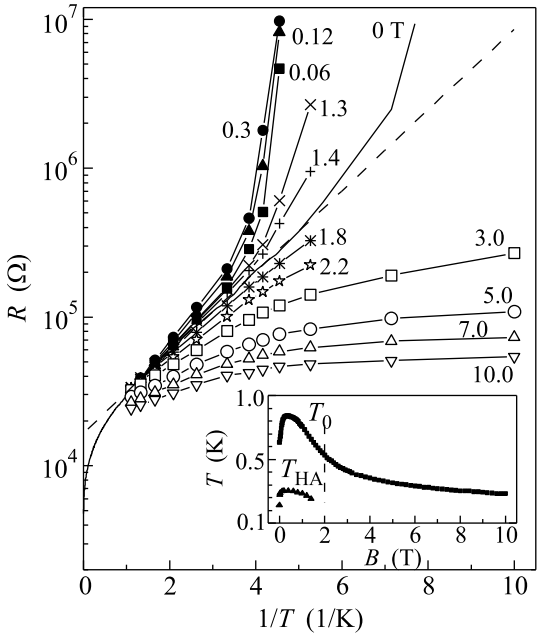

Fig.3. Arrhenius plots of the isomagnetic temperature dependences of the resistance of the insulating sample taken at fields B_i varying from 0 T to 10.0 T (the B_i are shown next to the respective curves). The inset: $T_0(B)$, the activation temperature extracted from $R(T, B_i)$ data in the temperature range 0.3–0.9 K. It assumes the maximum value 0.84 K at $B = 0.32$ T. $T_{\rm HA}(B)$ determined as explained in the text

and 21 kΩ). The nonmonotonic behavior of $T_0(B)$ resembles that of the magnetoresistance. At very lowest temperatures, however, the $\log R(1/T)$ plots deviate from the straight lines and diverge in a fan-like manner. To make the observed features even more transparent we have grouped the symbols for the data in Fig.3 into three branches. The solid symbols correspond to the temperature dependences taken within the *positive* magnetoresistance field window, i.e., at the magnetic fields $B_i < 0.32$ T. The 'crosses' correspond to fields B_i between 0.32 T and 2 T, at the negative slope of the peak. And, finally, open symbols denote isomagnetic temperature dependences at high fields $B_i > 2$ T, corresponding to the negative magnetoresistance tails. The zero field resistance is shown as a solid line, and the slope of the dashed line corresponds to the activation temperature at zero field. Figure 3 shows that in relatively small magnetic fields the resistance curves sharply jump upward from the Arrhenius activation behavior below some magnetic field dependent temperature $T_{\rm HA}(B)$. This hyperactivated behavior maintains till fields not exceeding 2 T. We define the characteristic temperature of the transition to the hyperactivated regime by the relation $R(T_{\rm HA}) = 2R_0 \exp(T_{\rm HA}/T_0)$, i.e., as the temperature at which the actually measured resistance exceeded two times the resistance obtained by extrapolation from the activated temperature interval. The inset in Fig.3 shows magnetic field dependence of $T_{\rm HA}(B)$ which appears nonmonotonic and looks similar to the field dependence of T_0. It is noteworthy that the hyperactivated regime exists on the both, positive- (solid symbols) and negative (crosses) magnetoresistance sides of the peak. Upon the further increasing magnetic field, the hyperactivation vanishes and is replaced by the *flattening* or downward deviation from the presumed activated behavior (open symbols). We emphasize here that the linearity of the $\log R(1/T)$ dependence in the 0.3 – 0.9 K window at fields beyond 3 T, can by no means be taken as an evidence of the thermally activated carrier transfer, since the activation temperatures that come out from fitting procedure are very close or even less than the lower bound of the observation interval, $T_0 \lesssim 0.3$ K. Moreover, the data in the whole temperature range $T < 0.9$ K and fields beyond 3 T are much better linearized in the $\log R$ versus $1/T^{1/2}$ representation. This suggests a recovery of the ES charge transfer mechanism at intermediate fields, which for the zero magnetic field was observed at $T > 0.6$ K. We find that upon increasing the magnetic field the ES characteristic temperature drops, whereas the preexponential factor increases, in particular, at $B = 3$ T, $T_{ES} = 1.8$ K and $R_1 = 6.8$ kΩ, and at $B = 10$ T, $T_{ES} = 0.39$ K and $R_1 = 12.6$ kΩ. This indicates that the ES VRH is suppressed by high magnetic fields (judging from decreasing T_{ES}) and that in the domain of the negative magnetoresistance the electron transfer which at moderated magnetic fields is mediated by Cooper pairs hopping, becomes quasiparticle dominated process at the elevated fields. We expect that upon further rise of the magnetic field the ES behavior changes to a metallic-like transport. At the same time, the behavior of the isotherms $R(B)$ of the insulating sample at high B resembles that of the superconducting samples from the Ref. [22], where it was described by the empirical relation $G(T, B) = 1/R_{\rm sat}(T) - \beta(T)\exp(-B/B^*)$, with B^* being some characteristic field, and with $R_{\rm sat}$ being close to the quantum resistance h/e^2. Following the same treatment as in [22], we present the $R(B)$ data in a similar scaling form as $G(B) = 1/R_{\rm sat} - 1/R(B)$ and plot it on a logarithmic scale as function of B (see Fig.4). Indeed, all the isotherms measured in the window from 900 mK down to 100 mK are well linearized via the proper choice of a single fitting parameter $R_{\rm sat}$ for each temperature (shown in the inset in Fig.4). The scaled $1/R(B)$ have the same temperature independent slope, corresponding to the characteristic field $B^* \simeq 11.2$ T, which is close to $B^* \simeq 10.7$ T for the sample A from Ref. [22].

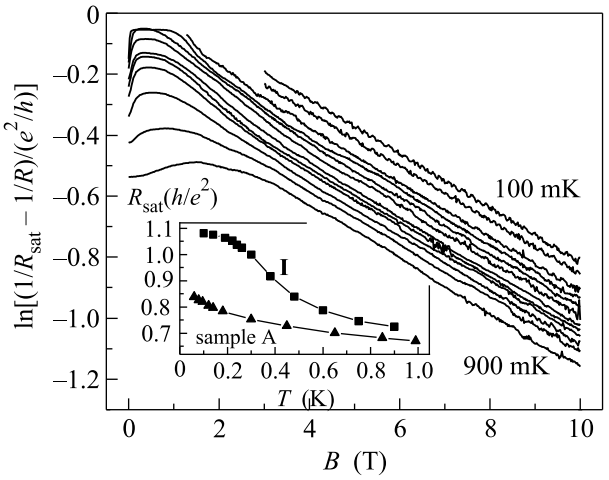

Fig.4. Scaling plot of the data shown in Fig.2: For certain values of R_{sat}, $\ln[1/R_{sat} - 1/R(B)]$ varies linearly vs. B, with a T-independent slope. The linear slope corresponds to the characteristic field $B^* \simeq 11.2$ T. Inset: Temperature dependence of R_{sat} for **I**-sample. We added data for superconducting sample A from Ref. [22]

We would like to complement our findings with the data on low temperature scanning tunneling spectroscopy measurements of the local density of states in the identically prepared TiN films [23]. It was found that even in comparatively less weakly disordered films, judging from the room temperature resistance, the superconducting state appears inhomogeneous. Furthermore, in spite of the fact, that the suppression of the superconducting transition temperature follows the fermionic mechanism [6], the analysis of the whole aggregate of the data supports the idea that the film in the critical region of the D-SIT can be viewed as an array of the superconducting islands immersed into an insulating sea or as a self-organized two-dimensional Josephson junction array [9, 13, 15, 19, 20, 24].

To gain an insight into the hyperactivation behavior from this standpoint, we juxtapose our data with the corresponding findings on granular films [25] and on two-dimensional Josephson junction arrays (2DJJ) [26 – 30]. These systems showed two distinct activated regimes with the different Arrhenius slopes. The smaller one is observed in the high fields and/or high temperature domain, where the superconductivity in the granules/superconducting electrodes was suppressed. In the low-T/low-B region, where granules/superconducting electrodes became superconducting, the Arrhenius activated curves acquired the *larger* slope. Specifically, in 2DJJ arrays, the activation energy in the "normal" state, which was found to be close to $(1/4)E_c$, where E_c was the charging energy of a single junction, increased to $(1/4)E_c + \Delta_0$, with Δ_0 being the gap of a superconducting electrode [26 – 28]. However, having decided to straightforwardly ascribe the upturn in $\log R$ versus $1/T$ dependences measured in our TiN films to opening the superconducting gap, we would have encountered immediate problems. Namely, using, for example, our data at $B = 0.06$ T, where the low temperature activation temperature as crudely estimated from the upturn is $T_0^l \simeq 6$ K, while at high temperatures $T_0 = 0.71$ K, we arrive at the magnitude of the opening gap to be of about 0.6 of that of the bulk TiN [31]. This is in strong conflict with the STM data of Ref. [23], where this ratio is estimated not to exceed 0.1 at the insulating side near the D-SIT.

Furthermore, having assumed that the observed upturn reflects the activation behavior, i.e. switching from a low activation energy to higher one we derive from the above analysis the nonphysically small pre-exponential factor, $R_0^l \approx 1.3 \cdot 10^{-5}\,\Omega$. This makes the notion of the activation transport at lowest temperatures in our films meaningless. On the other hand, Kanda and Kobayashi, and later Yamaguchi et al [29, 30], observed that the resistance of the 2DJJ array in the regime where electrodes are superconducting, increases, with decreasing temperature, faster than that of the thermal-activation type. They interpreted it as a signature of the charge binding-unbinding Berezinskii-Kosterlitz-Thouless (C-BKT) transition [32]. We propose that the hyperactivated behavior observed in our experiments is of the same nature and signalizes the formation of a low temperature C-BKT-phase, which we call a *superinsulator* [33, 34].

In conclusion, we have investigated the temperature- and the magnetic field dependences of the resistance of thin TiN films in the critical region of the disorder-driven superconductor-insulator transition. We have found that quantum metallicity, i.e. the saturation of high field negative magnetoresistance near the h/e^2 is a generic property of these films which belong not only to the superconducting- but also to the insulating side of the transition. At the same time, in the low perpendicular magnetic fields domain the thermally activated regime takes place at intermediate temperatures. At ultralow temperatures, the resistance becomes hyperactivated, i.e., grows faster than that of the thermally activated type. We relate the change of the mechanism of the conductivity with the charge binding-unbinding Berezinskii-Kosterlitz-Thouless transition and refer to the appearing low-temperature BKT-phase as to a superinsulating state. The conditions of formation of a superinsulating phase accounting for the role of the finite-size effects and the finite-range charge screening require further research.

We are grateful to A. Gerber for fruitful discussions. This research has been supported by the RFBR Grant No. 06-02-16704, the U.S. Department of Energy Office of Science through contract # DE-AC02-06CH11357, and the Deutsche Forschungsgemeinschaft within the GRK 638.

1. A. I. Shal'nikov, Nature (London) **142**, 74 (1938); A. I. Shal'nikov, Zh. Eksp. Teor. Fiz. **10**, 630 (1940).
2. M. Strongin, R. S. Thompson, O. F. Kammerer, and J. E. Crow, Phys. Rev. B **1**, 1078 (1970).
3. H. Raffy, R. B. Laibowitz, P. Chaudhari, and S. Maekawa, Phys. Rev. B **28**, 6607 (1983).
4. J. M. Graybeal and M. R. Beasley, Phys. Rev. B **29**, 4167 (1984).
5. S. Maekawa and H. Fukuyama, J. Phys. Soc. Jap. **51**, 1380 (1982).
6. A. M. Finkel'stein, Pis'ma v Zh. Eksp. Teor. Fiz. **45**, 37 (1987) [Sov. Phys. JETP Lett. **45**, 46 (1987)]; Physica B **197**, 636 (1994).
7. A. Gold, Z. Phys. B **52**, 1 (1983); Phys. Rev. A **33**, 652 (1986); Z. Phys. B **83**, 429 (1991).
8. M. P. A. Fisher, Phys. Rev. Lett. **65**, 932 (1990).
9. A. Ghosal, M. Randeria, and N. Trivedi, Phys. Rev. Lett. **81**, 3940 (1998); Phys. Rev. B **65**, 014501 (2001).
10. D. B. Haviland, Y. Liu, and A. M. Goldman, Phys. Rev. Lett. **62**, 2180 (1989).
11. Y. Liu, D. B. Haviland, B. Nease, and A. M. Goldman, Phys. Rev. B **47**, 5931 (1993).
12. D. Shahar and Z. Ovadyahu, Phys. Rev. B **46**, 10917 (1992).
13. D. Kowal and Z. Ovadyahu, Solid State Comm. **90**, 783 (1994).
14. J. J. Kim and H. J. Lee, Phys. Rev. Lett. **70**, 2798 (1993).
15. V. F. Gantmakher, M. V. Golubkov, J. G. S. Lok, and A. K. Geim, Zh. Eksp. Teor. Fiz. **109**, 1765 (1996) [JETP **82**, 951 (1996)].
16. G. Sambandamurthy, L. W. Engel, A. Johansson, and D. Shahar, Phys. Rev. Lett. **92**, 107005 (2004).
17. D. Kowal and Z. Ovadyahu, Physica C **468**, 322 (2008).
18. N. Hadacek, M. Sanquer, and J-C. Villégier, Phys. Rev. B **69**, 024505 (2004).
19. T. I. Baturina, A. Yu. Mironov, V. M. Vinokur et al., Phys. Rev. Lett. **99**, 257003 (2007).
20. T. I. Baturina, A. Bilušić, A. Yu. Mironov et al., Physica C **468**, 316 (2008).
21. B. L. Altshuler and A. G. Aronov, in: *Electron-Electron Interactions in Disordered Systems*, Eds. A. L. Efros and M. Pollak (North-Holland, Amsterdam, 1985.
22. T. I. Baturina, C. Strunk, M. R. Baklanov, and A. Satta, Phys. Rev. Lett. **98**, 127003 (2007).
23. B. Sacépé, C. Chapelier, T. I. Baturina et al., Phys. Rev. Lett. **101**, 157006 (2008).
24. Y. Imry, M. Strongin, and C. C. Homes, Physica C **468**, 288 (2008).
25. R. C. Dynes, J. P. Garno, and J. M. Rowell, Phys. Rev. Lett. **40**, 479 (1978).
26. T. S. Tighe, M. T. Tuominen, J. M. Hergenrother, and M. Tinknam, Phys. Rev. B **47**, 1145 (1993).
27. P. Delsing, C. D. Chen, D. B. Haviland et al., Phys. Rev. B **50**, 3959 (1994).
28. H. S. J. van der Zant, W. J. Elion, L. J. Geerligs, and J. E. Mooij, Phys. Rev. B **54**, 10081 (1996).
29. A. Kanda and S. Kobayashi, J. Phys. Soc. Jpn. **64**, 19 (1995).
30. T. Yamaguchi, R. Yagi, S. Kobayashi, and Y. Ootuka, J. Phys. Soc. Jpn. **67**, 729 (1998).
31. W. Escoffier, C. Chapelier, N. Hadacek, and J-C. Villégier, Phys. Rev. Lett. **93**, 217005 (2004).
32. R. Fazio and G. Schön, Phys. Rev. B **43**, 5307 (1991).
33. M. V. Fistul, V. M. Vinokur, and T. I. Baturina, Phys. Rev. Lett. **100**, 086805 (2008).
34. V. M. Vinokur, T. I. Baturina, M. V. Fistul et al., Nature **452**, 613 (2008).